International Journal of Mass Spectrometry 283 (2009) 94–99

Contents lists available at ScienceDirect

International Journal of Mass Spectrometry

journal homepage: www.elsevier.com/locate/ijms

Vibrational predissociation spectra of the O_n^-, $n = 3–10$, 12 clusters: Even–odd alternation in the core ion

Joseph C. Bopp, Anastassia N. Alexandrova, Ben M. Elliott, Tobias Herden, Mark A. Johnson*

Sterling Chemistry Laboratory, Yale University, P.O. Box 208107, New Haven, CT 06520, United States

ARTICLE INFO

Article history:
Received 17 December 2008
Received in revised form 3 February 2009
Accepted 4 February 2009
Available online 14 February 2009

Keywords:
Oxygen
Polaron
Anionic oxygen cluster
Vibrational predissociation
Core ion

ABSTRACT

We report vibrational predissociation spectra of the O_n^-, $n = 3–10$, 12 cluster ions in the 700–2400 cm^{-1} range. The odd numbered clusters are consistent with their identification as $O_3^- \cdot (O_2)_n$. The even numbered clusters are based on the O_4^- core ion, where the first two O_2 molecules add to O_4^- in locations that individually break the symmetry of the core ion, but together restore this symmetry. Beyond $O_4^- \cdot (O_2)_2$, subsequent O_2 attachment yields bands close to that of neutral O_2, indicating that the special character of the $O_4^- \cdot (O_2)_2$ cluster is retained.

1. Introduction

When a cluster consisting of closed shell molecules is electrically charged by either adding or removing an electron, the excess charge is accommodated on a smaller assembly consisting of 1–3 molecules, and this "core ion" is then effectively solvated by the remaining neutral molecules [1]. This is the cluster analogue of polaron formation in molecular solids [2]. The compositions of the core ions depend on both system and cluster size, and there are now many examples where the nature of the charge-bearing component has been identified using electronic [3,4,5], photoelectron [6–14], and most recently, vibrational spectroscopies [15–20]. The present work joins a number of recent contributions exploring homogeneous systems [18,19,21,22] using vibrational predissociation spectroscopy. Here we focus on the negatively charged clusters of oxygen, O_n^-, $n = 3–10$, and 12, which introduces the situation where the molecular constituents have an open shell electronic configuration.

The evolution of the O_n^- anions over the first few ($n = 1–4$) oxygen atoms occurs in a covalent bonding scenario in which all O atoms share the excess charge in the molecular orbital network. The $n = 2$ case is, of course, the diatomic superoxide [23–25] ion, while the $n = 3$ species is the C_{2v} ozonide anion [26,27]. The O_4^- ion provides the first non-trivial situation, where the resulting species is often regarded as a charge-resonance stabilized dimer derived from the degenerate $O_2^- \cdot O_2$ asymptotic structure, which has equal excess charge on both O_2 components. Two minimum energy O_4^- structures have actually been reported in the literature [16,28,29] with rectangular and trans-linear geometries. Vibrational spectroscopy established the presence of the rectangular structure [17,29], while a low-lying electronic band system near 4000 cm^{-1} has been interpreted as photoexcitation between the isomeric forms [16]. Photoelectron and photofragmentation spectra have been reported for the even clusters out to $n = 12$, and their photophysics has been analyzed in the context of a dimer core ion, O_4^- [30–35]. This conclusion is supported by thermochemical measurements of the incremental binding energies [33]. There are, on the other hand, no reports of the odd members of the O_n^- series above $n = 3$.

In this paper, we explore how the excess charge is accommodated when additional O_2 molecules are added to both the O_3^- and O_4^- species. Specifically, vibrational predissociation spectra are reported for the O_n^-, $n = 3–10$, 12 clusters in the 700–2400 cm^{-1} range using both Ar tagging and, when available, photofragmentation by loss of weakly bound O_2 molecules. The region of vibrational activity lies well below the adiabatic electron binding energies of all species relevant to this study [36]. To investigate the possible role of isomers, we performed electronic structure calculations utilizing the *ab initio* Gradient Embedded Genetic Algorithm (GEGA) and recovered a plethora of local minima. As it is generally difficult to distinguish extra bands arising due to anharmonicity from those corresponding to different isomers, we employed IR–IR hole burning [37] to identify experimentally the number of distinct species prepared by the supersonic jet ion source. The spectra indicate that

* Corresponding author. Tel.: +1 203 432 5226; fax: +1 203 432 6144.
E-mail address: mark.johnson@yale.edu (M.A. Johnson).

1387-3806/$ – see front matter © 2009 Elsevier B.V. All rights reserved.
doi:10.1016/j.ijms.2009.02.003

the odd numbered clusters form around the O_3^- core molecular anion, while the even clusters display extra bands that are traced to solvent-induced symmetry breaking in the O_4^- dimer core anion. Two isomers are identified for O_6^-, which both appear to be based on O_4^-.

2. Experimental methods

The larger O_n^-, n = 7–10, 12 clusters were generated by expanding pure oxygen gas at a stagnation pressure of about 3 bar and ionizing it with a counter-propagating 1 keV electron beam. The Ar tagged $O_n^- \cdot Ar$, n = 3–6 species were also surveyed, and were generated using the supersonic entrainment technique described previously [38] in which neat O_2 was introduced into a pure argon expansion through a second pulsed valve. In the case of ozonide and O_4^-, the Ar tagging method is essential since these ions are too stable (D_0 = 5110 and 3669 cm^{-1}, respectively) [27,33] to allow their vibrational fundamentals to be detected by predissociation in the one-photon absorption regime.

Vibrational predissociation spectroscopy was carried out with the Yale double-focusing, tandem time-of-flight photofragmentation spectrometer [32]. Tunable infrared radiation (700–2400 cm^{-1}) was generated using a Nd:YAG pumped OPO/OPA (Laser Vision) where parametric conversion in $AgGaSe_2$ delivered 3–300 μJ/pulse over the scan range, with the low power output occurring lowest in frequency. The reported spectra typically result from the accumulation of 5–10 individual scans, and are displayed as the net fragment ion yield normalized to the laser energy/pulse at each wavelength. The error in the reported wavenumbers of the bands is 5 cm^{-1} owing to the 2 cm^{-1} bandwidth of the laser and the reproducibility of the scans.

The search for the global minimum structures was performed using the Gradient Embedded Genetic Algorithm [39,40]. The initial search was done at the UB3LYP [41–43]/6-311G(d) [44,45] level. GEGA was run separately for clusters of multiplicities of 2, 4, 6, and 8. Subsequent CASSCF(7,8) [46–51]/6-311G(d) calculations revealed that all doublets and quartets have highly multiconfigurational wave functions. Therefore, all broken-symmetry UB3LYP solutions were corrected using the spin-projection procedure for the estimation of spin-coupling constants [52]. The energies of the final isomers were refined at the CCSD [53–58]/6-311G(d), CCSD/aug-cc-pVDZ, CASMRCI-SD [59,60]/6-311G(d) and CASMRCI-SD/aug-cc-pVDZ [61] levels. The UB3LYP, CASSCF, MPn, CCSD, and CCSD(T) were run using the Gaussian'03 [62] package. The CASMRCI-SD and CASPTn calculations were performed with the MOLPRO package [63].

We found that the even O_n^- clusters present several great challenges for theoretical treatment, which prevented us from their deeper exploration. Identified complications include: (1) their multiconfigurational nature; (2) the large electronic relaxation energies, making CASSCF results unreliable; (3) the failure of perturbation theory for these systems, which excludes the usage of such methods as MPn [64–68], CASPTn [69], and CCSD(T) [70] with triple excitations to be treated perturbatively; (4) the very flat and anharmonic potential energy surfaces, which, together with the failure of the perturbation theory, complicates calculation of their IR-spectra (e.g., results differ drastically between the methods, and also appear unacceptably blue shifted, as compared to the experiment); (5) problematic SCF-convergence (as can be anticipated); and (6) the fact that many isomers lie close in energy (11 isomers within 5 kcal/mol of the minimum energy structure), whose order also changes depending on the method. The most reliable protocol for treating these clusters would appear to be a complete geometry optimization at CASMRCI-SD along with analytic anharmonic frequency calculations; both of which, however, are presently computationally prohibitive. Thus, in spite of considerable effort, we can only provide a qualitative context for the likely structures at play in these clusters, and we report several minimum energy geometries lying close in energy using UB3LYP, CCSD, and CASMRCI-SD approaches. We explicitly note the nature of the difficulties here to alert future workers to some of the challenges presented by this surprisingly demanding system.

3. Results and discussion

3.1. Overview of the O_n^-, n = 3–10, 12 predissociation spectra

Fig. 1 presents an overview of the O_n^- vibrational predissociation spectra. This is a composite data collection, since the n = 3 and 4 spectra were obtained using Ar tagging while the $n \geq 5$ spectra correspond to loss of one or more O_2 molecules from the neat clusters. The number of O_2 molecules ejected gradually increases across the scan range as expected for the usual statistical fragmentation mechanism [20,71]. The dominant pattern in the spectra is an even/odd alternation in the location of a single intense feature, which appears near 800 cm^{-1} in the odd clusters and 1000 cm^{-1} in the even clusters. Several weaker bands appear in both cases which are spread out widely at higher energy. The chromophores arising from the O_3^- and O_4^- ions (dotted lines in Fig. 1) persist in the spectra of the odd and even series, respectively.

In the limiting cases of their characterizations as $O_3^- \cdot (O_2)_n$ and $O_4^- \cdot (O_2)_n$ cluster ions, one anticipates the possibility of observing vibrational excitation of the O_2 solvent molecules, especially in cases where asymmetric binding and/or moderate charge delocalization is at play [36]. The energy of the isolated O_2 fundamental (1568 cm^{-1}) [23,72] is indicated on the right side of Fig. 1, and

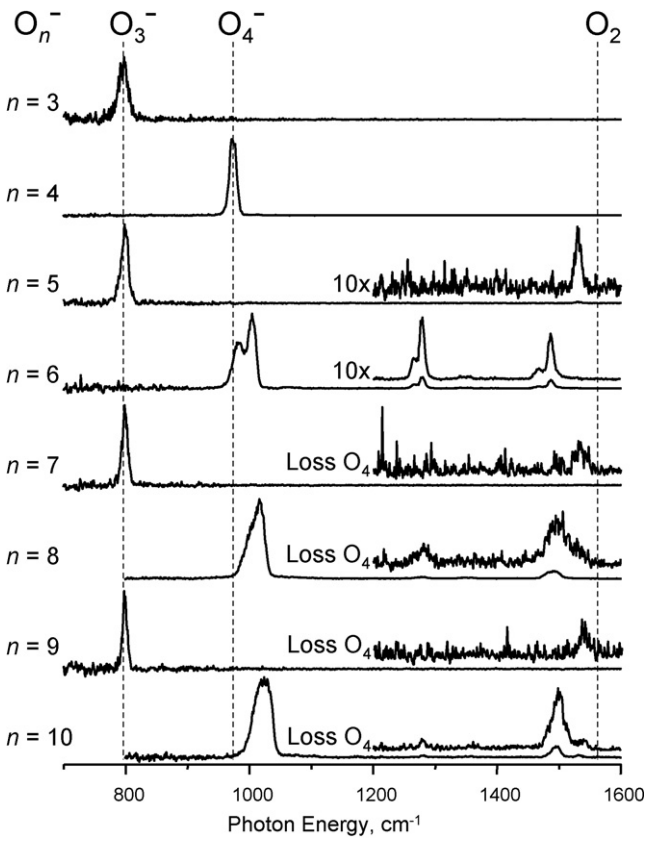

Fig. 1. Vibrational predissociation spectra of O_n^-, n = 3–10 clusters, employing both argon, n = 3–4, and O_2, n = 5–10, as messenger species. Dashed lines with labels denote the locations of bands for O_3^-, O_4^-, and O_2 at 797, 974, 1568 cm^{-1}, respectively. To reveal higher energy features for $n \geq 7$, spectra monitoring loss of O_4 are inset as this becomes the dominant loss channel at higher energies.

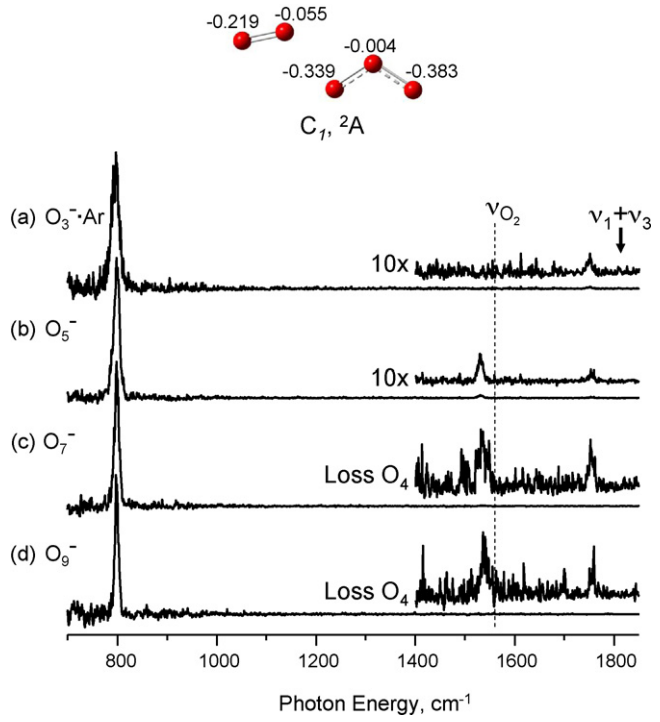

Fig. 2. Vibrational predissociation spectra of the odd O_n^- clusters, $n = 3$–9 in the 700–1850 cm^{-1} range. The infrared spectrum of $O_3^- \cdot Ar$ reveals transitions at 797 and 1752 cm^{-1}, which are assigned to the asymmetric stretch (ν_3) and a combination band of the asymmetric and symmetric stretches ($\nu_1 + \nu_3$), respectively. The expected location of this band, without accounting for anharmonicity, is indicated by the arrow. The neutral O_2 stretch (ν_{O_2}) is denoted by the dashed line. The structure corresponds to a low energy minimum recovered for the $O_3^- \cdots O_2$ cluster. The charges on the structure are the Natural Population Analysis [83–88] values computed at the B3LYP/6-311G(d) level of theory.

indeed $O_3^- \cdot O_2$ exhibits a weak band at 1531 cm^{-1} just below this value. On the other hand, the bands nominally associated with O_2 solvent molecules display a more complex evolution in the even clusters, as we discuss further below in Section 3.5. We first consider the simpler behavior of the odd clusters before discussing the origin of the band shifts and extra bands observed in the even analogues.

3.2. Band assignments in the $O_3^- \cdot (O_2)_n$ series

The dominant transition at 797 cm^{-1} recovered in $O_3^- \cdot Ar$ (Fig. 1a) is in excellent agreement with the antisymmetric stretching (ν_3) fundamental found at 796 cm^{-1} in a Ne matrix [29,73], and 804 cm^{-1} in an Ar matrix [74,75]. Fig. 2 isolates the spectra of the odd series to facilitate their direct comparison, and the locations of the observed transitions are collected in Table 1. The fact that this band is retained with very little perturbation in the larger clusters is consistent with the large difference between the electron affinities of O_3 and O_2 (2.103 and 0.448 eV, respectively) [76,77].

Table 1
Observed peak positions in the predissociation spectra of the O_n^-, $n = 3$, 5, 7, and 9, clusters.

Species	Observed transitions (cm^{-1})		
	ν_3	$\nu_{O_2}^{str}$	$\nu_1 + \nu_3$
$O_3^- \cdot Ar$[a]	797		1752
O_5^-	798	1531	1754
O_7^-	798	1535	1753
O_9^-	797	1539	1755

[a] Spectra obtained through the use of Ar atom as the "messenger" in the predissociation event.

Table 2
Observed peak positions in the predissociation spectra of the O_n^-, $n = 4$, 6, 8, 10, and 12, clusters.

Species	Observed transitions (cm^{-1})				
	ν_5	ν_1	$\nu_{O_2}^{str\ a}$	$\nu_{O_2}^{str\ b}$	$\nu_1 + \nu_5$
$O_4^- \cdot Ar$[c]	974				2231
O_6^-	982/1004	1266/1278	1468/1488		2230/2253
O_8^-	1016	1280	1492		2256
O_{10}^-	1024	1281	1499	1540	2267
O_{12}^-	1031		1500	1540	2278

[a] Peak corresponding to first solvation shell around the core ion.
[b] Peak corresponding to second solvation shell around the core ion.
[c] Spectra obtained through the use of Ar atom as the "messenger" in the predissociation event.

The features on the right side of Fig. 2 are expanded to highlight the behavior of the weaker transitions. The band arising from the O_2 solvent molecules occurs with a slight broadening and blue shift (~8 cm^{-1}) in going from $O_3^- \cdot O_2$ to $O_3^- \cdot (O_2)_3$.

To explore the origin of the infrared transition moment for excitation of the nominally forbidden O_2 fundamental, we carried out a search for minimum energy structures using the *ab initio* GEGA method, with the lowest energy structure included at the top of Fig. 2. The structure features asymmetrical attachment of the O_2 molecule to a terminal oxygen atom on the ozonide anion. The extent of asymmetry and charge transfer is indicated by the natural electron population analysis values included on the structure. Note that the structure shown is representative of a possible ground state, as various other multiplicities and geometries lie too close in energy to make a definitive determination of the ground state structure. In this structure, either vibration-induced modulation of charge transfer or the asymmetry induced in O_2 could activate the O_2 fundamental observed experimentally.

The $O_3^- \cdot (O_2)_n$ spectra also exhibit a weak feature higher in energy near 1750 cm^{-1}. This band is already present in the $O_3^- \cdot Ar$ spectrum (top trace in Fig. 2), establishing that it arises from the O_3^- core ion. Like the other bands observed in the odd clusters, it does not evolve significantly upon addition of O_2 molecules. The most straightforward assignment is to the $\nu_1 + \nu_3$ combination band, which is anticipated to occur, in the absence of anharmonicity, at 1815 cm^{-1} [78,79] as indicated by the arrow labeled $\nu_1 + \nu_3$ in Fig. 2. Such an assignment requires a X_{13} anharmonic coupling constant (−38 cm^{-1}) similar to that found in neutral O_3 (−31.4 cm^{-1}) [80]. Summarizing, the odd O_n^- clusters appear as a clear case where ozonide is simply surrounded by largely neutral O_2 "solvent" molecules.

3.3. Band assignments in the $O_4^- \cdot (O_2)_n$ series

Fig. 3 presents the spectra of even clusters, with expanded insets to highlight the weaker bands at higher energy. Locations of the observed transitions are collected in Table 2. The strong 974 cm^{-1} transition in O_4^- has also been reported in matrices [16,81] as well as in a previous study from our lab using Ar predissociation [17]. This band is due to the out-of-phase (b_{1u} symmetry) O–O stretching vibration of the two nearest O_2 moieties in rectangular O_4^- (see structure in inset), and is denoted ν_5 in the labeling scheme established by Jacox [29]. The large intensity of this transition is traced to the vibration-induced excess charge modulation associated with displacements along this mode, which alternately drive the system toward the more charge-localized $O_2^- \cdot O_2$ and $O_2 \cdot O_2^-$ electronic configurations. The characteristic O_4^- band is basically intact in the larger even clusters, consistent with the conclusion of the previous photoelectron and thermochemical studies that these are basically "dimer core" or $O_4^- \cdot (O_2)_n$ species [16,33]. The ~1000 cm^{-1} signature feature evolves into a close doublet in O_6^-,

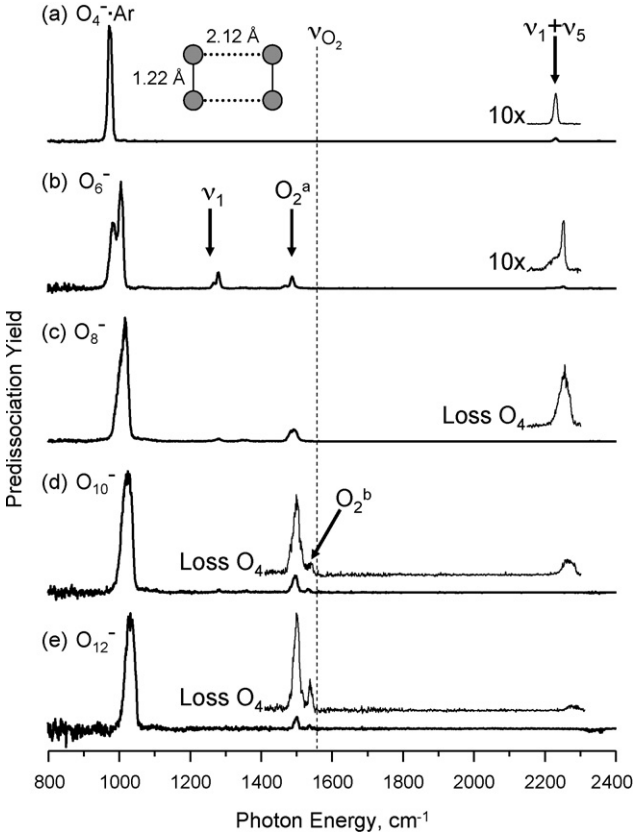

Fig. 3. Vibrational predissociation spectra of the even O_n^- clusters, n = 4–12 in the 800–2400 cm^{-1} range. For O_4^-, the feature at 974 cm^{-1} is assigned to the out of phase O_2 stretches (ν_5), while the feature at 2231 cm^{-1} is assigned to the $\nu_1 + \nu_5$ combination band of the in- and out-of-phase O_2 stretches. The free O_2 stretch is denoted by the dashed line. The labels O_2^a and O_2^b, indicate the signatures of the two distinct binding sites of the nominally neutral O_2 solvent molecules. The structure in (a) is taken from Ref. [28].

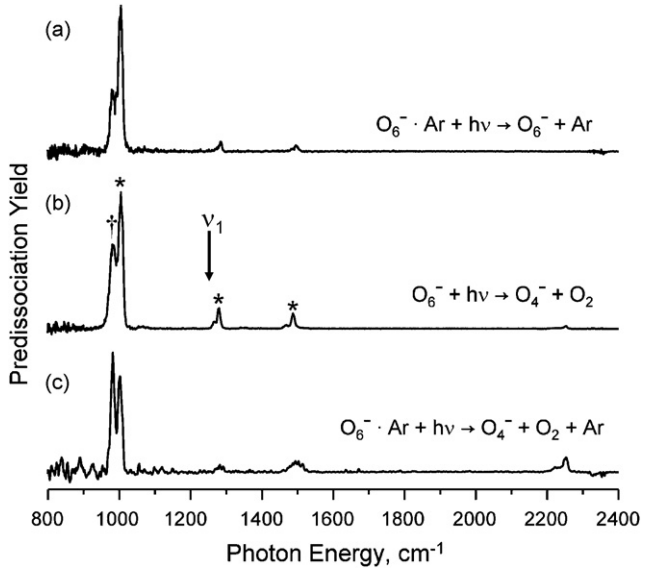

Fig. 4. Vibrational predissociation spectra of O_6^- collected using various predissociation pathways: (a) $O_6^- \cdot Ar$ collected through the loss of Ar, (b) bare, O_6^-, collected by the loss of O_2, and (c) $O_6^- \cdot Ar$ collected monitoring the loss of O_2 and Ar. The * in (b) indicate the features shown by double resonance to be associated with the same isomer, while the † indicates the member of the doublet belonging to a different isomer.

however, and broadens and blue shifts with increasing cluster size. These observations suggest that there is more interaction between the nominally neutral O_2 molecules and core ion than is apparent in the odd clusters.

A weak band is also evident at high energy in the Ar-solvated O_4^- ion (top trace) at 2231 cm^{-1}, which persists in the larger clusters. This band was observed previously [17] and assigned to a combination band of the rectangular O_4^- structure involving excitation of the ν_1, in-phase (Ag symmetry) stretching vibration of the two O_2 constituents along with one quantum of the ν_5 mode. Note that this band blue shifts with the stronger feature near 1000 cm^{-1} as O_2 molecules are added, supporting this assignment scheme where the upper band is linked to the lower energy transition. As mentioned earlier, the bands closest to the energy of the neutral O_2 transition (ν_{O_2}) are quite red-shifted for n = 6 and 8 (O_2^a), while a new band (O_2^b) appears closer to the neutral value at n = 10 and becomes stronger in the n = 12 spectrum.

Perhaps the most unexpected observation of this study is the evolution of the bands near the strong ν_5 band of O_4^- (~974 cm^{-1}) with additional O_2 molecules. This feature splits into a closely spaced (22 cm^{-1}) doublet in the O_6^- spectrum (Fig. 3b), and a new feature appears at 1278 cm^{-1} that was not present in the O_4^- spectrum.

3.4. A closer look at O_6^-: Ar tagging and isomer-selection using hole burning

The O_6^- spectrum presented in Fig. 3b was detected through photoejection of neutral O_2, and this presents a possible complication because the energy to remove one O_2 molecule from n = 6 is rather high (~840 cm^{-1}) [33] as determined from ion thermochemistry, and as such can possess significant internal energy. We therefore extended the study to include the $O_6^- \cdot Ar$ complex, because the argon atom has a lower binding energy than O_2, typically on the order of 400–500 cm^{-1} for small ions [82]. Fig. 4 presents a comparison of the bare O_6^- predissociation spectrum (Fig. 4b) with two action spectra obtained from the $O_6^- \cdot Ar$ complex that were recorded by monitoring the loss of Ar (Fig. 4a) and O_2 + Ar (Fig. 4c). The first conclusion from this comparison is that the features in the bare O_6^- spectrum persist in the Ar tagged species. Note, however, that the relative intensities of the bands differ according to whether the action spectra are recorded in the loss of Ar (40 amu, Fig. 4a) or O_2 + Ar (72 amu, Fig. 4c) fragmentation channels. It is, of course, usual to observe a gradual increase in the extent of fragmentation as the photon energy is increased on the scale of the binding energies for the species involved, as predissociation often occurs in the evaporative limit. This effect likely accounts for the appearance of the $\nu_1 + \nu_5$ band when detecting the loss of O_2 + Ar (Fig. 4c), which is absent when monitoring the loss of only Ar atoms (Fig. 4a). Such a mechanism cannot account for the strong intensity variations in the closely spaced doublet near 1000 cm^{-1}, however, as these transitions lie too close in energy (~22 cm^{-1}) to be significantly affected by their energetic difference. Nonetheless, the doublet appears with quite different relative intensities depending on the loss channel detected (0.85:1 in Fig. 4c and 2.5:1 in Fig. 4a). This behavior suggests that the two members of the doublet are derived from different isomeric species.

In order to sort out the role of isomers leading to heterogeneity of the O_6^- spectrum, we employed the pump-probe population labeling scheme recently developed in our laboratory to identify transitions arising from a common species [37]. In this approach, one laser is tuned to a particular transition to remove the population of the isomer responsible for it through predissociation, and a second laser is tuned through the spectrum to identify which transitions are depleted as one isomer is removed. This exercise demonstrated that all transitions labeled with (*) in Fig. 4b arise from the same isomeric species, while the lower energy member of

the doublet (labeled †) is indeed due to a second isomeric form. The differential loss behavior can then be understood if, for the † isomer, the effective binding energy for either the third O_2 molecule or the Ar atom (or both) is sufficiently lower relative to these values in the * isomer that the loss channel corresponding to ejection of O_2 and Ar is enhanced, even when the excited transition (†) occurs slightly lower in energy. Unfortunately, the shoulders on the lower energy side of the two bands occurring higher in energy near 1300 and 1500 cm^{-1} were too weak to allow identification using the double resonance technique. The proximity of the bands suggests that the two isomers have closely related structures.

3.5. Asymmetric solvation and importance of the $O_4^- \cdot (O_2)_2$ species

Having established that the strongest set of bands (* in Fig. 4) is due to one isomer, we now turn our attention to the assignment of the band at 1284 cm^{-1}, which only appears with appreciable intensity in the spectrum of O_6^-. We note that this energy is quite close to the value inferred for the ν_1 fundamental (arrow in Fig. 4b) based on the assignment of the $\nu_1 + \nu_5$ band at 2253 cm^{-1} (arrow in Fig. 3a). Recall that the ν_1 mode corresponds to the symmetrical (in-phase) stretching vibrations of the shortest O–O bonds in rectangular O_4^-, and is thus absent in the spectrum of O_4^- due to symmetry. The occurrence of this transition in O_6^-, along with the persistence of the O_4^- b_{1u} (ν_5) mode and the feature close to the O_2 stretch, all point to O_6^- adopting a structure with a O_4^- core ion solvated asymmetrically by a largely neutral O_2 molecule.

Regarding the nature of the isomer causing the feature marked † in Fig. 4b, we note that the extensive global minimum search performed during the GEGA runs shows that the potential energy surface corresponding to the motion of the third O_2 unit in O_6^- is extremely flat. Several of the minima arise from the O_2 molecule adopting a different orientation or location relative to the plane of the O_4^- rectangle. It is also possible that the second isomer could be due to another spin pairing in the cluster. For example, the calculations at various levels revealed that the O_6^- cluster has many low-lying spin states, and these minima often had nearly the same geometries, but occurred with the multiplicities raised or lowered relative to the minimum energy structure.

The assignment of an asymmetrical binding site (relative to the principle symmetry axes of the rectangle) for O_2 is supported by the behavior of the larger clusters. In particular, note that the ν_1 transition, which is quite distinct in O_6^-, becomes much smaller in the O_8^- spectrum. This suggests that the additional O_2 molecule adopts an equivalent binding site to that in $O_4^- \cdot O_2$, thus restoring symmetry and suppressing this band. Interestingly, the $O_4^- \cdot (O_2)_3$ spectrum (Fig. 3d) maintains the pattern of ν_5, $\nu_1 + \nu_5$ and $\nu_{O_2^a}$ but a new, weak transition appears that is closer to that of neutral O_2 (O_2^b in Fig. 3d), and this new peak becomes stronger in the $O_4^- \cdot (O_2)_4$ spectrum. The emerging overall picture is that the first two oxygen "solvent" molecules strongly attach to binding sites that perturb the core ion and yield O_2 bands with a significant red-shift (80 cm^{-1}). Once these two sites are filled, the symmetry of the core ion is restored, and subsequent O_2 molecules attach to more remote sites that yield bands closer to that of neutral O_2. This analysis refines the earlier conclusions of Hiraoka [33], which also indicated the enhanced stability of $O_4^- \cdot (O_2)_2$ in measurements of sequential binding energies of O_2 molecules onto O_2^-.

4. Conclusions

Vibrational predissociation spectra of the even numbered O_n^- clusters provide a more detailed picture of their structures than could be inferred from previous photophysical [34–36] and ion thermochemistry studies [33]. The persistence of the intense O_4^- bands in the higher clusters supports their earlier qualitative identification as $O_4^- \cdot (O_2)_n$ "dimer–core" complexes, but the vibrational bands indicate that the nominally neutral O_2 molecules add asymmetrically to the O_4^- core with two interactive binding sites that are signaled by red-shifts in the O–O stretching bands. The odd clusters are simpler in that they are accurately described as $O_3^- \cdot (O_2)_n$ clusters in which the ozonide ion is solvated by neutral O_2 molecules.

Acknowledgements

We thank the Chemistry Division of the National Science Foundation and the Air Force Office of Scientific Research for support of this work. ANA would like to thank Professor Boldyrev's group (Utah State University) for allowing the use of their computational resources for the GEGA runs.

References

[1] I. Becker, C.E.H. Dessent, M.A. Johnson, O. Cheshnovsky, Adv. Chem. Phys. 106 (1999) 265.
[2] M. Pope, C.E. Swenberg, Oxford University Press, New York, 1982.
[3] S. Barsotti, E. Leber, M.W. Ruf, H. Hotop, Int. J. Mass Spectrom. 220 (2002) 313.
[4] T. Tsukuda, M. Saeki, R. Kimura, T. Nagata, J. Chem. Phys. 110 (1999) 7846.
[5] C.E.H. Dessent, J. Kim, M.A. Johnson, J. Phys. Chem. 100 (1996) 12.
[6] R. Mabbs, E. Surber, L. Velarde, A. Sanov, J. Chem. Phys. 120 (2004) 5148.
[7] K. Pichugin, E. Grumbling, L. Velarde, A. Sanov, J. Chem. Phys 129 (2008) 044311.
[8] J.K. Song, S.Y. Han, I. Chu, J.H. Kim, S.K. Kim, S.A. Lyapustina, S. Xu, M. Nilles, K.H. Bowen Jr., J. Chem. Phys. 116 (2002) 4477.
[9] L.A. Posey, M.A. Johnson, J. Chem. Phys. 88 (1988) 5383.
[10] T. Tsukuda, T. Hirose, T. Nagata, Int. J. Mass Spectrom. Ion Processes 171 (1997) 273.
[11] M.J. DeLuca, B. Niu, M.A. Johnson, J. Chem. Phys. 88 (1988) 5857.
[12] T. Tsukuda, M.A. Johnson, T. Nagata, Chem. Phys. Lett. 268 (1997) 429.
[13] K.H. Bowen, J.G. Eaton, R.N.A.Z. in, Voger (Eds.), The Structure of Small Molecules and Ions, Plenum, New York, 1988, p. 147.
[14] T. Tsukuda, T. Hirose, T. Nagata, Chem. Phys. Lett. 279 (1997) 179.
[15] P.B. Comita, J.I. Brauman, J. Am. Chem. Soc. 109 (1987) 7591.
[16] J.A. Kelley, W.H. Robertson, M.A. Johnson, Chem. Phys. Lett. 362 (2002) 255.
[17] H. Schneider, J.M. Weber, E.M. Myshakin, K.D. Jordan, J. Bopp, T. Herden, M.A. Johnson, J. Chem. Phys. 127 (2007) 084319.
[18] J.-W. Shin, N.I. Hammer, M.A. Johnson, H. Schneider, A. Glob, J.M. Weber, J. Phys. Chem. A 109 (2005) 3146.
[19] T. Maeyama, T. Oikawa, T. Tsumura, N. Mikami, J. Chem. Phys. 108 (1998) 1368.
[20] M.A. Johnson, M.L. Alexander, W.C. Lineberger, Chem. Phys. Lett. 112 (1984) 285.
[21] R. Mabbs, E. Surber, A. Sanov, Chem. Phys. Lett. 381 (2003) 479.
[22] Y. Kobayashi, Y. Inokuchi, T. Ebata, J. Chem. Phys. 128 (2008) 164319.
[23] C.G. Bailey, D.J. Lavrich, D. Serxner, M.A. Johnson, J. Chem. Phys. 105 (1996) 1807.
[24] R.J. Celotta, R.A. Bennett, J.L. Hall, M.W. Siegel, J. Levine, Phys. Rev. A 6 (1972) 631.
[25] M.J. Travers, D.C. Cowles, G.B. Ellison, Chem. Phys. Lett. 164 (1989) 449.
[26] M.E. Jacox, D.E. Milligan, J. Mol. Spectrosc. 43 (1972) 148.
[27] S.E. Novick, P.C. Engelking, P.L. Jones, J.H. Futrell, W.C. Lineberger, J. Chem. Phys. 70 (1979) 2652.
[28] A.J.A. Aquino, P.R. Taylor, S.P. Walch, J. Chem. Phys. 114 (2001) 3010.
[29] W.E. Thompson, M.E. Jacox, J. Chem. Phys. 91 (1989) 3826.
[30] P.C. Cosby, R.A. Bennet, J.R. Peterson, J.T. Moseley, J. Chem. Phys. 63 (1975) 1612.
[31] D.C. Conway, L.E. Nesbitt, J. Chem. Phys. 48 (1968) 509.
[32] L.A. Posey, M.J. DeLuca, M.A. Johnson, Chem. Phys. Lett. 131 (1986) 170.
[33] K. Hiraoka, J. Chem. Phys. 89 (1988) 3190.
[34] D.H. Paik, T.M. Bernhardt, N.J. Kim, A.H. Zewail, J. Chem. Phys. 115 (2001) 612.
[35] K.A. Hanold, A.K. Luong, R.E. Continetti, J. Chem. Phys. 109 (1998) 9215.
[36] M.J. DeLuca, C.C. Han, M.A. Johnson, J. Chem. Phys. 93 (1990) 268.
[37] B.M. Elliott, R.A. Relph, J.R. Roscioli, J.C. Bopp, G.H. Gardenier, T.L. Guasco, M.A. Johnson, J. Chem. Phys. 129 (2008) 094303.
[38] W.H. Robertson, J.A. Kelley, M.A. Johnson, Rev. Sci. Instrum. 71 (2000) 4431.
[39] A.N. Alexandrova, A.I. Boldyrev, J. Chem. Theor. Comp. 1 (2005) 566.
[40] A.N. Alexandrova, A.I. Boldyrev, Y.J. Fu, X. Yang, X.B. Wang, L.S. Wang, J. Chem. Phys. 121 (2004) 5709.
[41] R.G. Parr, W. Yang, Oxford University Press, Oxford, 1989.
[42] A.D. Becke, J. Chem. Phys. 98 (1993) 5648.
[43] J.P. Perdew, J.A. Chevary, S.H. Vosko, K.A. Jackson, M.R. Pederson, D.J. Singh, C. Fiolhais, Phys. Rev. B 46 (1992) 6671.
[44] T. Clark, J. Chandrasekhar, G.W. Spitznagel, PvR. Schleyer, J. Comp. Chem. 4 (1983) 294.
[45] M.J. Frisch, J.A. Pople, J.S. Binkley, J. Chem. Phys. 80 (1984) 3265.
[46] D. Hegarty, M.A. Robb, Mol. Phys. 38 (1979) 1795.
[47] R.H.A. Eade, M.A. Robb, Chem. Phys. Lett. 83 (1981) 362.
[48] H.B. Schlegel, M.A. Robb, Chem. Phys. Lett. 93 (1982) 43.
[49] F. Bernardi, A. Bottoni, J.J.W. Mcdouall, M.A. Robb, H.B. Schlegel, Far. Symp. Chem. Soc. 19 (1984) 137.

[50] N. Yamamoto, T. Vreven, M.A. Robb, M.J. Frisch, H.B. Schlegel, Chem. Phys. Lett. 250 (1996) 373.
[51] M. Frisch, I.N. Ragazos, M.A. Robb, H.B. Schlegel, Chem. Phys. Lett. 189 (1992) 524.
[52] L. Noodleman, J. Chem. Phys. 74 (1981) 5737.
[53] J. Cizek, Adv. Chem. Phys. 14 (1969) 35.
[54] J.A. Pople, R. Krishnan, H.B. Schlegel, J.S. Binkley, Int. J. Quantum Chem. 14 (1978) 545.
[55] G.D. Purvis, R.J. Bartlett, J. Chem. Phys. 76 (1982) 1910.
[56] R.J. Bartlett, G.D. Purvis, Int. J. Quantum Chem. 14 (1978) 516.
[57] G.E. Scuseria, C.L. Janssen, H.F. Schaefer, J. Chem. Phys. 89 (1988) 7382.
[58] G.E. Scuseria, H.F.S. III, J. Chem. Phys. 90 (1989) 3700.
[59] H.-J. Werner, P.J. Knowles, J. Chem. Phys. 82 (1985) 5053.
[60] P.J. Knowles, H.-J. Werner, Chem. Phys. Lett. 115 (1985) 259.
[61] D.E. Woon, T.H. Dunning Jr., J. Chem. Phys. 98 (1993) 1358.
[62] Gaussian 03, Revision C.02, M.J. Frisch, G.W. Trucks, H.B. Schlegel, G.E. Scuseria, M.A. Robb, J.R. Cheeseman, J.J.A. Montgomery, T. Vreven, K.N. Kudin, J.C. Burant, J.M. Millam, S.S. Iyengar, J. Tomasi, V. Barone, B. Mennucci, M. Cossi, G. Scalmani, N. Rega, G.A. Petersson, H. Nakatsuji, M. Hada, M. Ehara, K. Toyota, R. Fukuda, J. Hasegawa, M. Ishida, T. Nakajima, Y. Honda, O. Kitao, H. Nakai, M. Klene, X. Li, J.E. Knox, H.P. Hratchian, J.B. Cross, V. Bakken, C. Adamo, J. Jaramillo, R. Gomperts, R.E. Stratmann, O. Yazyev, A.J. Austin, R. Cammi, C. Pomelli, J.W. Ochterski, P.Y. Ayala, K. Morokuma, G.A. Voth, P. Salvador, J.J. Dannenberg, V.G. Zakrzewski, S. Dapprich, A.D. Daniels, M.C. Strain, O. Farkas, D.K. Malick, A.D. Rabuck, K. Raghavachari, J.B. Foresman, J.V. Ortiz, Q. Cui, A.G. Baboul, S. Clifford, J. Cioslowski, B.B. Stefanov, G. Liu, A. Liashenko, P. Piskorz, I. Komaromi, R.L. Martin, D.J. Fox, T. Keith, M.A. Al-Laham, C.Y. Peng, A. Nanayakkara, M. Challacombe, P.M.W. Gill, B. Johnson, W. Chen, M.W. Wong, C. Gonzalez, J.A. Pople, Gaussian, Inc., Wallingford, CT, 2004.
[63] MOLPRO, version 2006.1, a package of *ab initio* programs, H.-J. Werner, P. J. Knowles, R. Lindh, F. R. Manby, M. Schütz, P. Celani, T. Korona, A. Mitrushenkov, G. Rauhut, T. B. Adler, R.D. Amos, A. Bernhardsson, A. Berning, D.L. Cooper, M.J.O. Deegan, A.J. Dobbyn, F. Eckert, E. Goll, C. Hampel, G. Hetzer, T. Hrenar, G. Knizia, C. Köppl, Y. Liu, A. W. Lloyd, R.A. Mata, A.J. May, S.J. McNicholas, W. Meyer, M.E. Mura, A. Nicklass, P. Palmieri, K. Pflüger, R. Pitzer, M. Reiher, U. Schumann, H. Stoll, A.J. Stone, R. Tarroni, T. Thorsteinsson, M. Wang, A. Wolf, see http://www.molpro.net, 2006.
[64] C. Moller, M.S. Plesset, Phys. Rev. 46 (1934) 618.
[65] M. Head-Gordon, J.A. Pople, M.J. Frisch, Chem. Phys. Lett. 153 (1988) 503.
[66] M.J. Frisch, M. Head-Gordon, J.A. Pople, Chem. Phys. Lett. 166 (1990) 275.
[67] M.J. Frisch, M. Head-Gordon, J.A. Pople, Chem. Phys. Lett. 166 (1990) 281.
[68] S. Saebo, J. Almlof, Chem. Phys. Lett. 154 (1989) 83.
[69] H.J. Werner, Mol. Phys. 89 (1996) 645.
[70] J.A. Pople, M. Head-Gordon, K. Raghavachari, J. Chem. Phys. 87 (1987) 5968.
[71] P.J. Campagnola, L.A. Posey, M.A. Johnson, J. Chem. Phys. 95 (1991) 7998.
[72] G. Herzberg, Van Nostrand Reinhold Company Inc., New York, 1950.
[73] C.L. Lugez, W.E. Thompson, M.E. Jacox, J. Chem. Phys. 105 (1996) 2153.
[74] L. Andrews, B.S. Ault, J.M. Grzybowski, R.O. Allen, J. Chem. Phys. 62 (1975) 2461.
[75] C.A. Wight, B.S. Ault, L. Andrews, J. Chem. Phys. 65 (1976) 1244.
[76] D.W. Arnold, C.S. Xu, E.H. Kim, D.M. Neumark, J. Chem. Phys. 101 (1994) 912.
[77] K.M. Ervin, W. Anusiewicz, P. Skurski, J. Simons, W.C. Lineberger, J. Phys. Chem. A 107 (2003) 8521.
[78] R.C. Spiker, L. Andrews, J. Chem. Phys. 59 (1973) 1851.
[79] L. Andrews, R.C. Spiker, J. Chem. Phys. 59 (1973) 1863.
[80] A. Barbe, A. Chichery, T. Cours, V.G. Tyuterev, J.J. Pleteaux, J. Mol. Struct. 616 (2002) 55.
[81] G.V. Chertihin, L. Andrews, J. Chem. Phys. 108 (1998) 6404.
[82] A. Wada, A. Kikkawa, T. Sugiyama, K. Hiraoka, Int. J. Mass Spectrom. 267 (2007) 284.
[83] J.E. Carpenter, F. Weinhold, J. Mol. Struct. Theochem. 169 (1988) 41.
[84] J.P. Foster, F. Weinhold, J. Am. Chem. Soc. 102 (1980) 7211.
[85] A.E. Reed, F. Weinhold, J. Chem. Phys. 78 (1983) 4066.
[86] A.E. Reed, F. Weinhold, J. Chem. Phys. 83 (1985) 1736.
[87] A.E. Reed, R.B. Weinstock, F. Weinhold, J. Chem. Phys. 83 (1985) 735.
[88] A.E. Reed, L.A. Curtiss, F. Weinhold, Chem. Rev. 88 (1988) 899.